Brain Struct Funct (2008) 212:481–495
DOI 10.1007/s00429-008-0195-z

ORIGINAL ARTICLE

The human inferior parietal lobule in stereotaxic space

Svenja Caspers · Simon B. Eickhoff · Stefan Geyer · Filip Scheperjans · Hartmut Mohlberg · Karl Zilles · Katrin Amunts

Received: 6 May 2008 / Accepted: 11 July 2008 / Published online: 24 July 2008

Abstract Recently, a new cytoarchitectonic map of the human inferior parietal lobule (IPL) has been proposed, with the IPL consisting of seven cytoarchitectonically distinct areas (Caspers et al. in Neuroimage 33(2):430–448, 2006). The aim of the present study was to investigate the different aspects of variability of these IPL areas. As one aspect of variability, we analysed the topographical relationship between the localisation of the borders of the areas and macroanatomical landmarks. Although five areas occupy the surface supramarginal gyrus and two the angular gyrus, their borders cannot be reliably detected by means of macroanatomy. To account for variability in size and extent of the areas in stereotaxic space, cytoarchitectonic probabilistic maps have been calculated for each IPL area. Hemisphere- and gender-related differences have been investigated on basis of volumes of cytoarchitectonic areas. For one of them, area PFcm, a significant gender difference in volume was found with males having larger volumes than females; this difference exceeds that of gender differences in total brain volume. The different aspects of variability and volumetric asymmetry may underlie some of the well-known functional asymmetries in the IPL, observed, for example during fMRI experiments analysing spatial attention or motor attention, and planning. The cytoarchitectonic probabilistic maps of the seven IPL areas provide a robust anatomical reference and open new perspectives for further structure–function investigations of the human IPL.

Keywords Cytoarchitecture · Human brain mapping · Parietal cortex · Volumetry · Lateralization · Gender · Intersubject variability

S. Caspers (✉) · S. B. Eickhoff · F. Scheperjans · H. Mohlberg · K. Zilles · K. Amunts
Research Centre Jülich, Institute of Neurosciences and Biophysics—Medicine, 52425 Jülich, Germany
e-mail: s.caspers@fz-juelich.de

S. Geyer · K. Zilles
C. and O. Vogt Institute for Brain Research, Heinrich-Heine-University Düsseldorf, 40001 Düsseldorf, Germany

K. Zilles · K. Amunts
JARA, Research Centre Jülich, Institute of Medicine, 52425 Jülich, Germany

K. Amunts
Department of Psychiatry and Psychotherapy, RWTH Aachen University, 52074 Aachen, Germany

Introduction

Brodmann (1909) subdivided the human inferior parietal lobule (IPL) into a rostral area BA 40, occupying the supramarginal gyrus, and a caudal area BA 39, located on the angular gyrus. This parcellation has recently been revised (Caspers et al. 2006), based on an observer-independent cytoarchitectonic analysis (Zilles et al. 2002; Schleicher et al. 2005). Seven cytoarchitectonic areas were identified (Fig. 1). Five of them (PFop, PFt, PF, PFm, and PFcm) approximately covered the region of BA 40 on the supramarginal gyrus with extension into the depth of the Sylvian fissure, the remaining two areas (PGa and PGp) were located approximately at the position of BA 39 on the angular gyrus.

The aim of the present study was to investigate different aspects of variability of these areas, i.e. intersubject, interhemispheric, and gender differences. One aspect of variability relates to the topography of the areas. Previous studies (Amunts et al. 1999, 2000, 2005; Caspers et al. 2006; Choi et al. 2006; Eickhoff et al. 2006a; Geyer 2004;

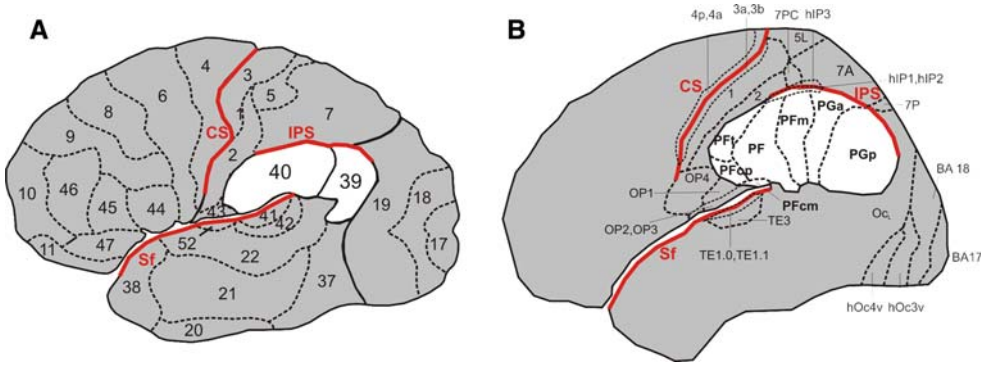

Fig. 1 **a** Schematic drawing of a lateral view of Brodmann's brain map and **b** of the IPL areas as provided by the new parcellation (Caspers et al. 2006) and of surrounding areas as published (areas 4a, 4p: Geyer et al. 1996; area 1, 3a, 3b: Geyer et al. 2000; area 2: Grefkes et al. 2001; areas OP1–OP4: Eickhoff et al. 2006a; areas 5L, 7PC, 7A, 7P, hIP3: Scheperjans et al. 2008; area TE1–TE3: Morosan et al. 2001; BA17, BA18: Amunts et al. 2000; hOc3v, hOc4v: Rottschy et al. 2007); Oc_L: lateral occipital cortex (yet unmapped). IPL areas are highlighted in *white*. In *red*: *Sf* Sylvian fissure, *CS* central sulcus, *IPS* intraparietal sulcus

Geyer et al. 1996, 2000; Grefkes et al. 2001; Morosan et al. 2001; Malikovic et al. 2007; Rottschy et al. 2007; Scheperjans et al. 2008) demonstrated that macroanatomical landmarks such as gyri and sulci predict the location of cytoarchitectonic borders with sufficient precision only for a few cortical regions, e.g. primary somatosensory and motor cortex. Therefore, one of the aims of the present study was to provide a topographical characterisation of the IPL areas with respect to sulci and gyri, and surrounding cortical areas. We calculated the frequencies for such relationships as an estimate of the intersubject variability.

Cytoarchitectonic probabilistic maps for each IPL area in stereotaxic space were generated in order to quantify the intersubject variability in the T1-weighted, single subject reference brain of the Montreal Neurological Institute (MNI space; Evans et al. 1992; Collins et al. 1994; Holmes et al. 1998). These maps allow the assignment of each voxel of the reference space to a specific brain area (Amunts et al. 2007a; Zilles et al. 2002). Information about the interindividual variability of inferior parietal areas was not provided in the 'classical' brain maps of Brodmann (1909), Vogt and Vogt (1919), von Economo and Koskinas (1925), Gerhardt (1940), Sarkissov et al. (1955) and Batsch (1956). Furthermore, the former brain maps represented only schematic views of a brain in 2-D print format. Probability maps contain true 3-D information. Thus, they do not only consider superficially located areas, but also parts of the cortex, which are hidden in the depth of sulci. The consideration of these cortical regions is important, since two-third of the total cortical surface spread into the sulci (Zilles et al. 1988). Probability maps of the IPL are, therefore, a more reliable and precise tool for the localisation of results from functional imaging experiments in order to analyse structure–function relationships, than the classical brain maps and the atlas of Talairach and Tournoux (1988), which is based on Brodmann's schematic drawing of a map.

A further focus of analysis was put on interhemispheric asymmetry and gender differences in the IPL areas. Functional imaging studies reported such differences in the past. For example, attention reorientation is lateralized to the right, whereas motor attention and planning are more left-lateralized (e.g. Astafiev et al. 2003; Corbetta and Shulman 2002; Hesse et al. 2006; Rushworth et al. 2001a, b). These results are supported by clinical findings: left-sided IPL lesions were associated with apraxia and Wernicke's aphasia, whereas right-sided lesions most often caused neglect (e.g. Abo et al. 2004; Blank et al. 2002; Fink and Heide 2004; Halligan et al. 2003; Jodzio et al. 2003; Kerkhoff 2001; Marshall et al. 2001; Vallar 2001). The reported results for gender differences in lesion studies were contradictory: whereas some studies reported differences in neurological symptoms between males and females in dependence on the extent of the lesion (e.g. Lang and Moser 2003; Kimura 1983), others did not (e.g. Kertesz and Benke 1989; Lendrem and Licoln 1985; Miceli et al. 1981). In healthy subjects, gender differences in the IPL were observed for affective arousal, movement planning and cognitive control (e.g. Bell et al. 2006; Boghi et al. 2006; Smith et al. 1987).

Based on these data the question arises whether and to what extent such functional differences are reflected on a structural level. Thus, we analysed the volumes of all IPL areas as one putative feature of IPL anatomy, contributing to interhemispheric and gender differences.

Materials and methods

Cytoarchitectonic probability maps

The seven cytoarchitectonic areas of the IPL have been identified in serial histological sections of ten human post-

mortem brains based on an observer-independent approach for detecting significant changes in cortical lamination pattern (Caspers et al. 2006; Schleicher et al. 2005). The brains have been obtained from the body donor program of the Department of Anatomy, University of Düsseldorf, Germany (Table 1). Subjects had no known history of neurological or psychiatric diseases. The brains have been dehydrated in graded alcohols, and embedded in paraffin. Coronal whole-brain sections were obtained using a large-scale microtome (section thickness 20 μm). On basis of MR-images of the brains, histological sections were 3-D reconstructed (Caspers et al. 2006).

The extent of cytoarchitectonic areas of the IPL was traced in serial high-resolution images (resolution of the digitized images: 7,000 × 6,000 pixels, 21.2 μm per pixel) of serial histological sections using the KS400 system (Zeiss, Germany), and in-house software (Amunts et al. 2007b). Using affine and nonlinear elastic registration and employing a multiscale approach (Hömke 2006), these images together with the labelled cytoarchitectonic areas were registered to the 'anatomical MNI space' as reference space (Amunts et al. 2005). In contrast to the 'original' T1-weighted MNI single subject brain (Evans et al. 1992; Collins et al. 1994; Holmes et al. 1998), the anatomical MNI space aligns the brain data sets to the anterior commissure at the level of the interhemispheric fissure as the origin (0, 0, 0). The 'anatomical' MNI space differs from the 'original' MNI space by a linear shift of the origin (4 mm more caudally (y axis), and 5 mm more dorsally (z axis)).

After registration to the common reference space, the corresponding areas from each brain were superimposed, and probabilistic maps were calculated for each IPL area. The maps indicate for each voxel of the reference brain the relative frequency, with which a respective area was found at that position. A probability of 10% indicates a position, where an area was found in only one individual brain out of ten. A probability of 100% indicates that an area was found in all ten brains. Probability information was supplemented by the corresponding centres of gravity for each probability map.

Table 1 Brains used for cytoarchitectonic analysis of the IPL areas

Brain no.	Age	Cause of death	Gender
14/94	43	Pulmonary embolism	Female
2/95	85	Mesenteric artery infarction	Female
382/81	59	Cardiorespiratory failure	Female
68/95	79	Cardiorespiratory failure	Female
71/86	86	Cardiorespiratory failure	Female
16/96	54	Myocardial infarction	Male
139/95	74	Myocardial infarction	Male
146/86	37	Right heart failure	Male
207/84	75	Toxic glomerulonephritis	Male
2431	39	Drowning	Male

The probabilistic cytoarchitectonic maps of different areas might overlap to some extent. In one voxel, for example, one particular area might be found with a probability of 60%, whereas two other areas might be found with a probability of 20% each. For visualisation and comparison with functional data, an unambiguous assignment of each voxel to one and only one area is meaningful. The maximum probability map (MPM) represents such a non-overlapping parcellation of the human brain and the IPL, in particular (Eickhoff et al. 2005, 2006b). The advantage of an MPM is, that it reflects volumes and locations of cytoarchitectonic areas more precisely than other methods, which are based on simple thresholding of the original probability maps (Eickhoff et al. 2006b). The MPM was calculated by assigning each voxel of the reference space to the most likely area at its position. If two areas showed the same probability at a particular voxel, this voxel was assigned to the area with the higher average probabilities in directly adjacent voxels. If, in some cases, a definite allocation could still not be achieved, the described procedure was repeated on probability maps smoothed by an isotropic 6 mm Gaussian kernel (Eickhoff et al. 2005).

The MPM which was calculated for the present study includes the IPL areas as well as surrounding areas: primary and premotor cortex (areas 4a, 4p, 6; Geyer et al. 1996, 2004), primary somatosensory cortex (areas 3a, 3b, 1, 2; Geyer et al. 2000; Grefkes et al. 2001), secondary somatosensory cortex (areas OP1–OP4; Eickhoff et al. 2006b), primary auditory cortex (areas TE 1.0, TE 1.1, TE 3; Morosan et al. 2001), anterior ventral bank of the intraparietal sulcus (areas hIP1, hIP2; Choi et al. 2006), primary and secondary visual cortex (areas 17, 18, hOc3v, hOc4v, hOc5; Amunts et al. 2000; Rottschy et al. 2007; Malikovic et al. 2007) and subcortical structures (hippocampus, amygdala, entorhinal cortex; Amunts et al. 2005).

For each IPL area, histograms of the distribution of the cytoarchitectonic probabilities have been calculated. These histograms are based on the normalised and affine, and nonlinear elastic registered data of the ten examined brains. Therefore, they reflect the cytoarchitectonic probability distribution in MNI space.

Stereotaxic and volumetric analysis of IPL areas

For each IPL area, the centre of gravity in the 3-D reference space was calculated. Interhemispheric differences between the stereotaxic coordinates of the centres of gravity were investigated by using a pairwise permutation test, separately for each axis of 3-D space. In a first step, the 20 centres of gravity (ten for each hemisphere) were grouped according to their origin (left or right hemisphere, respectively).

Between the means of these groups, a contrast estimate for the main effect of hemisphere was calculated. In a second step, the 20 values were randomly assigned to the two groups. This procedure was iterated 1,000,000 times to provide a non-parametric estimate of the null distribution for each contrast. Differences between two areas were considered to be significant if the contrast estimate of the true comparison was larger than 95% of the values of the null distribution ($P < 0.05$) (see also Scheperjans et al. 2008). Intersubject variability in the stereotaxic location was quantified by calculating the standard deviations (SD) of the centres of gravity coordinates for each area.

For the volumetric analysis, the high-resolution images with delineated IPL areas (see above) were used. Depending on the rostro-caudal extent of the IPL, up to 25 of these images were analysed per hemisphere. Based on the delineations, the volume of each IPL area was calculated as.

$$V = s \times T \times x \times y \times \sum A_i \times F \quad (1)$$

where V is the volume of the cortical area in mm^3, s is the number of sections between two measured sections (60), T is the thickness of a section (20 μm), x is the width of a pixel (21.2 μm), y is the height of a pixel (21.2 μm), ΣA_i is the area (in pixels) across all i evaluated sections, and F is the individual shrinkage factor of each post-mortem brain. The shrinkage correction considered that several steps of histological tissue processing such as dehydration in graded alcohols and embedding in paraffin led to tissue shrinkage. The correction factors were calculated according to Amunts et al. (2005). The corrected absolute volumes were analysed for hemispheric and gender differences using a similar pairwise permutation test as described above for the stereotaxic analysis.

To quantify the variability of the volumetric data, the variation coefficient (CV) was calculated:

$$\mathrm{CV} = \mathrm{SD}/\mathrm{mean} \quad (2)$$

where "mean" is the mean volume of each IPL area, averaged over all examined brains and SD is the standard deviation. By means of the variation coefficient, an appraisal of volume variability in different areas was possible. Lower values of the variation coefficient indicated higher stability of the corresponding volumes across the ten examined brains.

Results

Topography of IPL areas in relation to anatomical landmarks and surrounding areas

The relationships to macroanatomical landmarks and neighbouring areas were variable among the areas (Table 2).

The two most rostral areas, PFop and PFt (Fig. 1), shared a common border in all hemispheres. In 9 of 20 hemispheres, PFop was found most rostrally; in 6 hemispheres, area PFt was the most rostral one. In the remaining 5, both areas ended approximately at the same rostro-caudal level. Area PFop often reached into the Sylvian fissure, but was rarely buried completely within the sulcus (2/20). PFop always had common borders with the areas of the parietal operculum, the SII cortex (OP1–OP4, Eickhoff et al. 2006c), most consistently with areas OP1 and OP4 (Table 2). Since area OP2 was located deeper within the Sylvian fissure, it was separated from PFop by OP1 in all cases but one.

Area PFt, in contrast, was always located on the free surface of the supramarginal gyrus, and occupied parts of the posterior bank of the postcentral sulcus (Figs. 1, 5). It bordered BA 2 (Grefkes et al. 2001) in 19 hemispheres (Table 2). In only six hemispheres, PFt reached into the Sylvian fissure. In four of these six hemispheres, PFt bordered the SII cortex within the Sylvian fissure, namely areas OP4 and OP1 (Table 2). That is, in the remaining two hemispheres additional, yet uncharted, architectonic areas were located within the Sylvian fissure between PFt and OP1/OP4.

Area PF was located caudally to PFt on the free surface of the supramarginal gyrus. Dorso-ventrally, it extended from the intraparietal sulcus (IPS) to the Sylvian fissure. Posterior to the caudal end of the Sylvian fissure, the ventral border of PF was located at the temporo-parietal junction (Figs. 1, 5). In four cases, PF spread onto the superior temporal gyrus (Table 2). PF always bordered PFt, PFm and PFcm, and mostly also PFop. Among the areas extending into the IPS, i.e. PF, PFm, PGa, and PGp, area PF was the most rostral one. In the IPS, PF often shared a common border with intraparietal area hIP2 (Choi et al. 2006) in more than 50% of the hemispheres (13/20).

PFcm was located caudally to PFop on the upper bank of the Sylvian fissure and ventrally to PF on the inferior part of the supramarginal gyrus, sometimes reaching its free surface (Figs. 1, 5). Normally, PFcm shared a common border with area PF, only in two hemispheres also with area PFm. Anteriorly, PFcm bordered PFop most frequently (17/20). Less consistent, PFcm bordered the SII cortex, mainly area OP1 (Table 2).

Area PFm was located caudally to PF, mainly on the supramarginal and only partly on the angular gyrus (Figs. 1, 5). PFm always reached into the IPS and, in contrast to area PF, also spread onto its ventral bank in seven hemispheres, though never onto its dorsal bank. In the IPS, PFm frequently bordered the anterior intraparietal areas hIP1 and hIP2 (Choi et al. 2006; see Table 2). PFm always bordered the rostral area of caudal IPL, area PGa. These areas, therefore, marked the border between rostral

Table 2 Relationship of the IPL areas to surrounding areas and macroanatomical landmarks in ten post-mortem brains ($n = 20$ hemispheres)

	Number of hemispheres		Number of hemispheres
PFop		*PFcm*	
Free surface	18	OP1	11
Sylvian fissure	17	OP2	2
OP4	10	PFop	17
OP1	19	PF	20
OP2	1	PFm	2
BA2	6	Free surface	6
Reaching most rostrally	9		
PFt		*PFm*	
Sylvian fissure (ventral margin of IPC)	6	hIP2	11
OP4	3	hIP1	13
OP1	1	PF	20
PFop	20	PGa	20
PF	20	PFcm	2
BA2	19	IPS (dorsal margin of IPC)	20
hIP2	3	IPS (depth)	7
Dorsal bank of poc	12		
Reaching most rostrally	6		
PF			
hIP2	13		
hIP1	2		
PFcm	20		
PFm	20		
PFop	14		
BA2	1		
OP1	3		
IPS (dorsal margin of IPC)	20		
IPS (depth)	0		
PGa	3		
Superior temporal gyrus	4		
PGa		*PGp*	
hIP2	2	hIP2	0
hIP1	10	hIP1	0
PF	3	IPS (dorsal margin of IPC)	20
PFm	20	IPS (depth)	4
IPS (dorsal margin of IPC)	20	PGa	20
IPS (depth)	6	hOc5	0

Areas are named as published: BA2 (Grefkes et al. 2001); hIP1, hIP2 (Choi et al. 2006), OP1–OP4 (Eickhoff et al. 2006c); PFop, PFt, PF, PFm, PFcm, PGa, PGp (Caspers et al. 2006); hOc5 (Malikovic et al. 2007). IPC inferior parietal cortex, IPS intraparietal sulcus without hIP1, hIP2; poc postcentral sulcus. "Free surface" and "Sylvian fissure" mean, that the area reaches the free surface or the Sylvian fissure, respectively, whereas its major part is located in the depth of the sulcus

and caudal IPL areas, approximately between BA 40 and BA 39.

Caudally, area PFm was followed by area PGa, which was located on the angular gyrus. PGa always extended into the depth of the IPS (Figs. 1, 5). It sometimes covered parts of its ventral bank, bordering hIP1 and hIP2, though less frequently than areas PF and PFm (Table 2). Like areas PF and PFm, PGa also bordered yet unmapped parts of the IPS. An approximate landmark for its ventral extent was the caudal end of the superior temporal sulcus. Caudally, area PGa always shared a common border with PGp. This border was mostly located in the depth of the angular sulcus (the dorsal continuation of the superior temporal sulcus).

Area PGp, finally, was the most caudal area of the IPL (Fig. 1). It never extended into the Sylvian fissure. However, similar to areas PF, PFm, and PGa, PGp reached into the IPS (Fig. 5). In contrast to these areas, area PGp never shared a common border with the anterior intraparietal areas hIP1 and hIP2. The caudal extent of

PGp usually coincided with the continuation of the anterior occipital sulcus at the caudal margin of the angular gyrus. The ventral extension of PGp was rather variable, but always located dorsally to the inferior temporal sulcus. If the anterior occipital sulcus, as the posterior end or the superior segment of a double parallel superior temporal sulcus, was connected to the end of the superior temporal sulcus (which can be found, according to Ono et al. (1990), in 40% of the right and 52% of the left hemispheres), this connection between these two sulci provided a landmark for the ventro-caudal margin of PGp. Area PGp was surrounded by cortex, which has not been cytoarchitectonically mapped so far by our own group. In the map of Brodmann (1909), such parts of the cortex were labelled as BA 19 (occipital lobe) and BA 37 (temporal lobe). At the caudal borders of PGp, area hOc5 of the visual cortex (Malikovic et al. 2007) was visible on the same slices, but did not border area PGp directly.

Probabilistic maps and intersubject variability in stereotaxic space

Topographical variability in stereotaxic space was further quantified by calculating probability maps for each IPL area (Figs. 2, 3).

High probabilities, i.e. where a particular area was present in eight or more of ten brains, were found in a relatively small amount of voxels. Low probabilities (i.e. 10–30%) were observed in a considerably larger number of voxels. The distributions of probability values (histograms) have been calculated for each IPL area and are shown in Fig. 4.

The probability maps and their corresponding probability distributions reflect the interindividual variability of the respective area. In all IPL areas except for right PFop, voxels with an overlap of at least 80% were observed in both hemispheres (Fig. 4), i.e. the respective area was located in at least eight of ten brains in these voxels. An exception was found for area PFop in the right hemisphere, which only reached a maximal overlap of 60% (Fig. 4b). In the left hemisphere, only area PF and in the right hemisphere, only areas PF, PFm, PGa, and PGp reached an overlap of 100% in a few voxels, i.e. in a magnitude of a few hundred voxels (cf. Figs. 2, 3, 4). The probability distributions of the IPL areas in the left hemisphere resembled each other more than those in the right hemisphere.

Although all IPL areas showed a considerable variability, they differed between each other in degree. Larger areas, like PF, PFm, PGa, and PGp, showed less variability (i.e. more overlap at high probabilities) than smaller areas, like PFop, PFt, and PFcm (see Fig. 4).

The considerable amount of intersubject variability caused an overlap between probability maps of neighbouring areas. One and the same voxel in the MNI reference space can be occupied by the probability maps of two adjacent areas, in particular by their low probability parts. In order to account for such overlap and to achieve an unambiguous presentation of different cytoarchitectonic probability maps, an MPM has been calculated for all IPL and surrounding areas (Fig. 5).

The MPM is a tool to visualise the topographical relationships between the IPL areas and to surrounding areas as the primary and secondary somatosensory cortex (areas 3a, 3b, 1, BA 2, OP1–OP4), intraparietal areas hIP1 and hIP2, and extrastriate area hOc5. The centres of gravity of the areas in the MPM were located within one standard deviation of the centres of gravity of the respective probability maps (Table 3; see also Eickhoff et al. 2005).

Another aspect of the interindividual variability was related to the stereotaxic coordinates of the IPL areas. Hereby, the most interesting values were the y coordinates and their variation, as the IPL areas were mainly ordered in a rostro-caudal sequence, i.e. showed differences in their y values (Fig. 6).

Accordingly, the results of pairwise permutation test for the stereotaxic coordinates showed significant differences between most of the areas in the y values ($P < 0.05$). Only the y coordinates of the two ventral areas, PFop and PFcm, did not differ significantly from those of their dorsal neighbours (areas PFt and PF, respectively). However, PFop and PFt on the one hand, and PFcm and PF on the other hand were arranged in a ventro-dorsal sequence, and their z coordinates differed between each other ($P < 0.05$). The variability of the stereotaxic coordinates as judged by SD was comparable for x, y, and z values (see Fig. 6a, b for x, and y coordinates). Comparing the variability of the coordinates in all IPL areas, no significant difference was found either; the stereotaxic location of all IPL areas was relatively stable in all spatial directions.

Volumetric analysis

Intersubject variability

Another aspect of variability was approached by comparing the volumes of the cytoarchitectonic areas. The volumes of all IPL areas varied considerably between different brains, for both smaller (areas PFop, PFt, and PFcm) and larger areas (areas PF, PFm, PGa, and PGp; Table 4).

As an example of a larger area, the volume of area PF varied between 1,510 and 4,420 mm^3 in the left, and between 1,449 and 3,245 mm^3 in the right hemisphere.

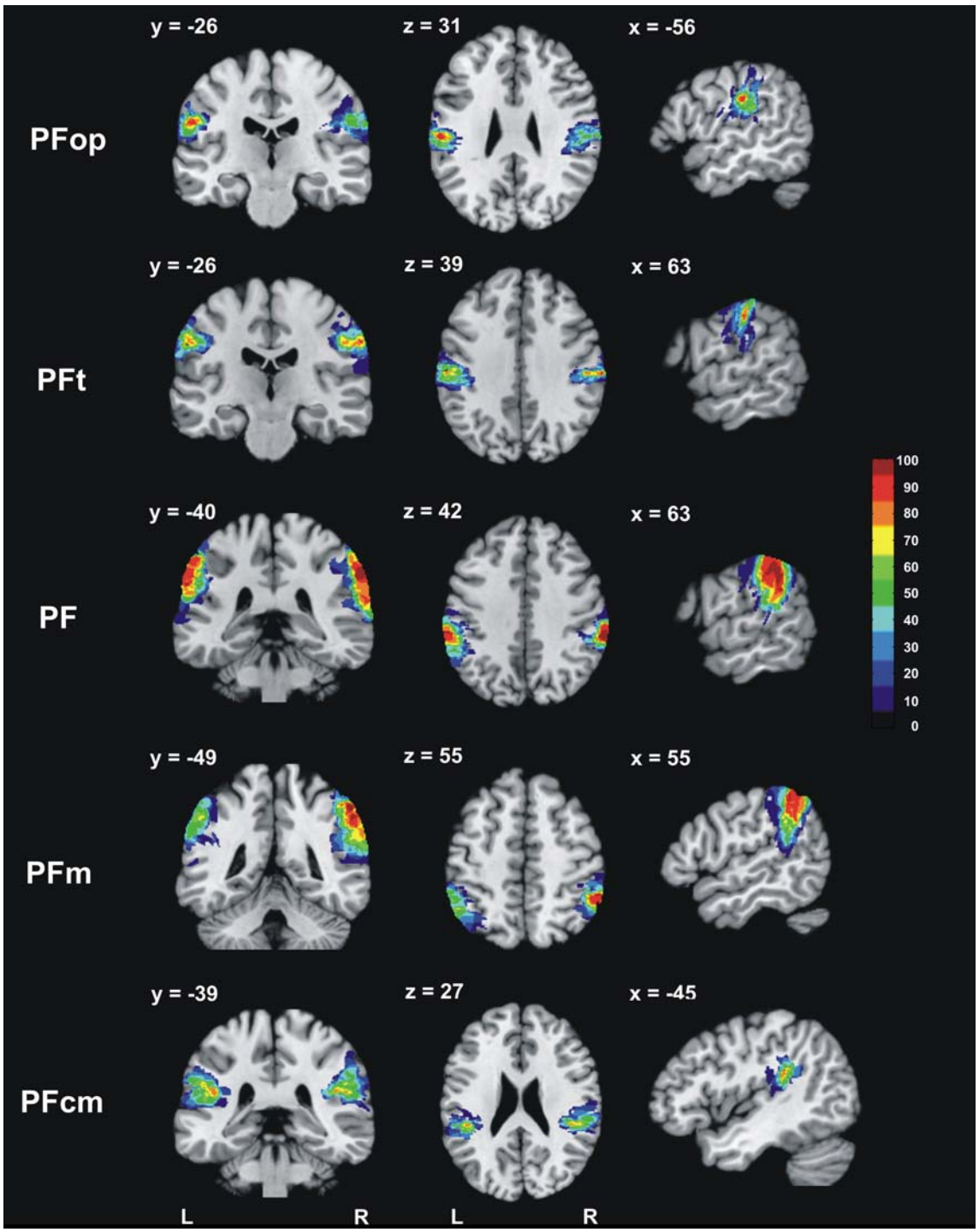

Fig. 2 Orthogonal sections through the anatomical MNI single subject template, showing probability maps of rostral IPL areas PFop, PFt, PF, PFm, and PFcm (according to BA 40), displayed in three planes (*left to right columns*: coronal (*y* axis), horizontal (*z* axis), sagittal (*x* axis). Negative *x* values correspond to the left hemisphere, positive to the right hemisphere. Colour map encodes low probabilities in dark blue (one out of ten brains, 10%) up to high probabilities in *dark red* (ten out of ten brains, 100%). *L*, *R* left and right hemispheres, respectively

The volume of area PFop, an example of a smaller area, varied between 418 and 1,667 mm^3 in the left, and between 475 and 1,855 mm^3 in the right hemisphere. The other areal volumes varied in a comparable amount. This variability was reflected by the variation coefficients for all areas: the variability was minimal for area PGa with

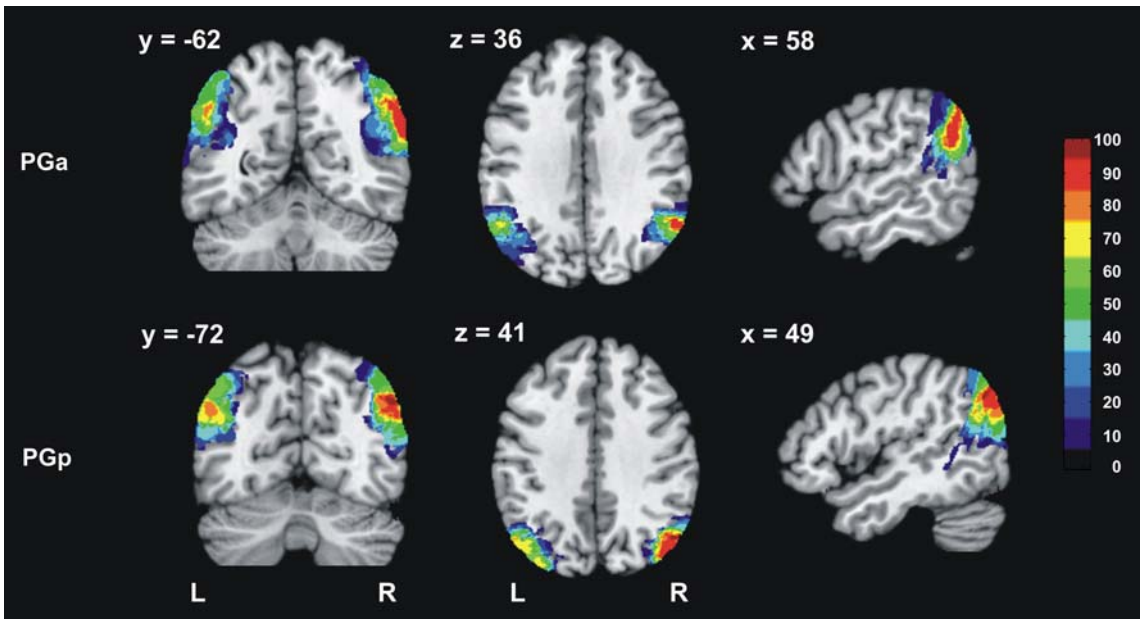

Fig. 3 Orthogonal sections through the MNI single subject template, showing the probability maps of caudal IPL areas PGa and PGp (according to BA 39). Designations as in Fig. 2

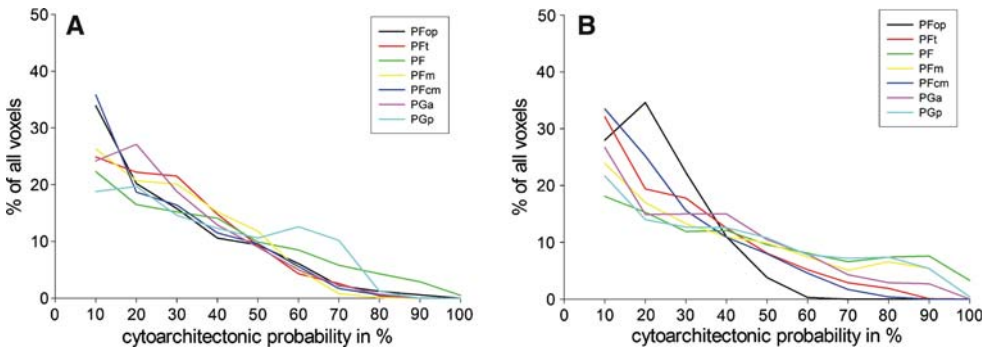

Fig. 4 Percentage of voxels plotted against the cytoarchitectonic probability from 10% (one of ten brains) to 100% (ten of ten brains) for all IPC areas in the left (**a**) and right hemisphere (**b**). The graphs show the probability distributions in one probability map as an aspect of intersubject variability. The steeper the curve the higher variable *i* respective area

variation coefficients of 0.23 and 0.25 in left and right hemisphere, respectively, and maximal for areas PFop in the right and PFcm in the left hemisphere with a variation coefficient of 0.51 (Table 4). The results showed that the volumes of the smaller areas tended to be more variable than those of the larger areas, which were more stable, at least for the mean volumes, irrespective of gender or gender–side interaction.

Gender and interhemispheric differences

The volumes were further tested for significant gender differences and hemispheric asymmetry (Fig. 7). The permutation test showed that area PFcm, which was located in the Sylvian fissure, differed significantly between males and females with male PFcm having a larger volume than female PFcm by a factor of 1.8 ($P < 0.001$). At the same time, the mean total volume of male brains in this study was larger than that of female brains by a factor of 1.2 (Amunts et al. 2007b). Thus, the gender difference in area PFcm was greater than expected on the basis of brain size alone. For area PFm, the volumes in male brains were also significantly larger than in female brains ($P < 0.05$; factor 1.3). This difference, however, resembled that of brain size. The gender specific volume data, separately for left and right hemispheres, are given in Table 5.

The IPL areas of the left and the right hemispheres did not differ between each other in volume (Fig. 7).

The gender- and hemisphere-specific variation coefficients are shown in Fig. 7b. With a few exceptions, the larger areas tended to be less variable than the smaller ones, irrespective of gender or hemisphere. However, the variation coefficient for the volume of female PFop in left hemispheres, an example of a smaller area, was relatively small, whereas the variation coefficients for the volume of male PGp and female PF in the left hemisphere, as examples of larger areas, showed high values.

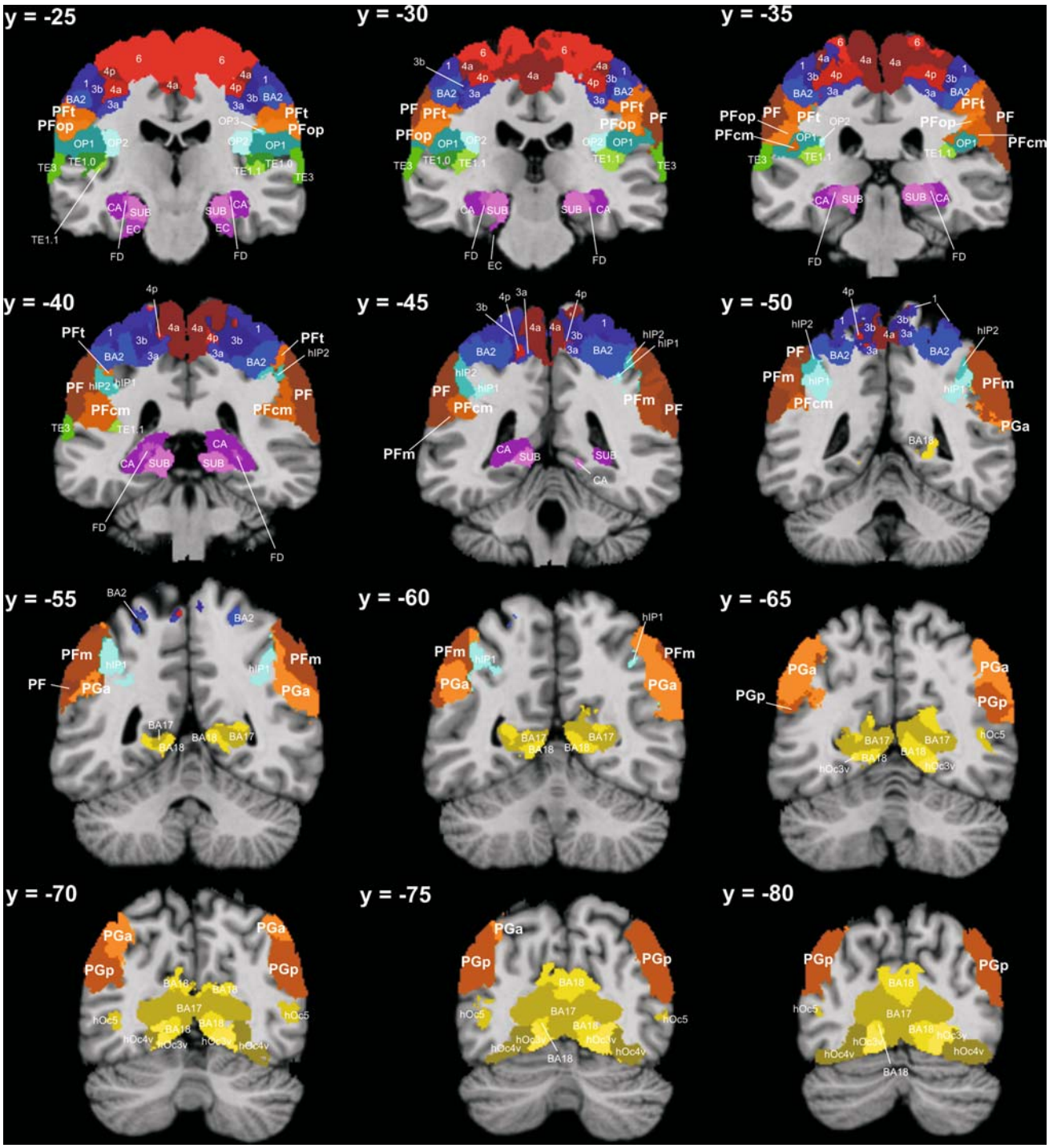

Fig. 5 Sequence of coronal sections (every 5th from $y = -25$ to $y = -80$) of the MNI single subject template, showing the maximum probability maps (MPM) of the IPL (shades of *brown* and *orange*) and surrounding areas as labelled. Shades of *red*: primary (areas 4a, 4p, Geyer et al. 1996) and premotor cortex (area 6, Geyer 2004), shades of *blue*: primary somatosensory cortex (areas 3a, 3b, 1, Geyer et al. 2000; BA 2, Grefkes et al. 2001), shades of *light blue*: secondary somatosensory cortex (areas OP1-4, Eickhoff et al. 2006c), shades of *green*: primary auditory cortex (areas TE 1.0, TE 1.1, TE 3, Morosan et al. 2001), shades of *lilac*: hippocampus (areas of *FD* fascia dentate, *CA* cornu ammonis, *EC* entorhinal cortex, *SUB* subiculum; Amunts et al. 2005), shades of *turquoise*: areas on the anterior ventral bank of the intraparietal sulcus (areas hIP1, hIP2, Choi et al. 2006), shades of *yellow* and *olive*: visual cortex (areas BA 17, BA 18, Amunts et al. 2000; hOc3v, hOc4v, Rottschy et al. 2007; hOc5, Malikovic et al. 2007)

Table 3 Coordinates of the centres of gravity of the IPL areas after nonlinear normalisation in anatomical MNI space

Area	Type of map	Left hemisphere			Right hemisphere		
		x	*y*	*z*	*x*	*y*	*z*
PFop	Prob. map	−57 ± 2.9	−26 ± 5.9	31 ± 4.7	56 ± 3.7	−24 ± 6.1	31 ± 5.7
	MPM	−57	−30	30	55	−26	32
PFt	Prob. map	−54 ± 2.9	−29 ± 4.9	43 ± 6.3	55 ± 4.5	−29 ± 3.9	45 ± 6.6
	MPM	−52	−29	40	53	−31	44
PF	Prob. map	−57 ± 2.1	−41 ± 5.5	41 ± 4.3	61 ± 1.9	−38 ± 2.9	38 ± 4.8
	MPM	−58	−43	39	62	−39	35
PFm	Prob. map	−53 ± 4.3	−54 ± 6.7	44 ± 6.1	55 ± 1.6	−49 ± 3.8	45 ± 5.7
	MPM	−52	−56	45	54	−50	42
PFcm	Prob. map	−51 ± 2.8	−39 ± 3.6	30 ± 4.7	53 ± 2.8	−36 ± 4.2	30 ± 5.3
	MPM	−49	−42	28	51	−38	29
PGa	Prob. map	−46 ± 5.8	−65 ± 6.7	43 ± 5.2	52 ± 3.5	−59 ± 2.9	39 ± 7.2
	MPM	−46	−65	44	51	−60	38
PGp	Prob. map	−43 ± 3.9	−76 ± 6.0	37 ± 4.8	47 ± 3.0	−73 ± 4.1	38 ± 6.7
	MPM	−43	−78	35	46	−75	34

Data for left and right hemispheres

Mean values (±standard deviation, SD) based on mapping in ten post-mortem brains. MPM show the coordinates of the centre of gravity of the respective area's representation in the maximum probability map (Eickhoff et al. 2006b)

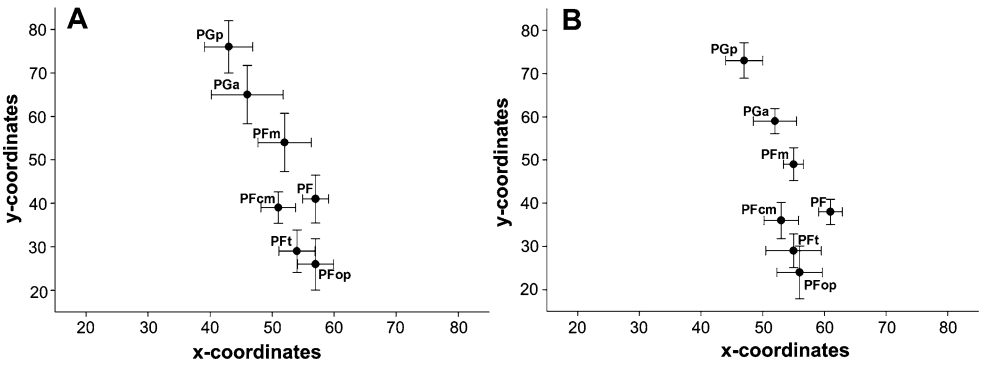

Fig. 6 Scatter plots of centres of gravity of cytoarchitectonic areas with *y* coordinates plotted against *x* coordinates for left (**a**) and right hemisphere (absolute values for the *x* coordinates) (**b**). Corresponding standard deviations as *horizontal* (for *x*) and *vertical* (for *y*) bars. All coordinate values are given in anatomical MNI space

Discussion

The present study was focused on different aspects of intersubject variability of cytoarchitectonic areas on the human inferior parietal lobule. It provided an analysis of the topographical relationship of the areas to each other, to neighbouring cortical areas as well as to macroanatomical landmarks such as the intraparietal sulcus and the Sylvian fissure. Probabilistic maps of all IPL areas quantified the intersubject variability in the anatomical MNI reference space. Hence, cytoarchitectonic data of the IPL are now available in a format, which can directly be matched to the results of in vivo functional neuroimaging studies. Structural–functional comparisons provide the opportunity to understand the intersubject variability, which has been measured during functional imaging experiments involving the parietal lobe (e.g. Chung et al. 2007; Tzourio-Mazoyer et al. 2004; Sugiura et al. 2007; Vesia et al. 2006), in more detail. Gender and hemispheric differences for volumetric as well as for stereotaxic data are features, which may contribute to anatomical intersubject variability.

Intersubject topographical differences

The macrostructure of the brain, i.e. the pattern of sulci and gyri, and its relationship to the borders of cortical areas may vary independently. Macroanatomical landmarks of the IPL represent in some, but not all cases an estimate of the position of a cytoarchitectonic area. Several parietal areas seemed to 'prefer' certain areal neighbours and sulci. The four large areas on the free inferior parietal surface (areas PF, PFm, PGa, and PGp), for example, always reached the IPS. Thus, the IPS marked the approximate position of the dorsal border of these areas. Areas hIP1 and

Table 4 Volumetric data of the IPL areas

	Left hemisphere	Right hemisphere
PFop	941 ± 329.5	915 ± 468.0
CV	0.35	0.51
PFt	1,430 ± 584.3	1,454 ± 572.8
CV	0.41	0.39
PF	2,891 ± 1175.3	2,492 ± 592.8
CV	0.41	0.24
PFm	2,363 ± 939.1	2,356 ± 648.8
CV	0.40	0.28
PFcm	1,041 ± 531.1	979 ± 399.2
CV	0.51	0.41
PGa	2,666 ± 677.1	2,830 ± 644.6
CV	0.25	0.23
PGp	2,884 ± 1,182.6	3,221 ± 1,150.0
CV	0.41	0.36

Mean volumes (±standard deviations) in mm^3 and variation coefficients (CV) for each IPL area. Individual correction for shrinkage due to histological processing has been performed according to Amunts et al. (2005)

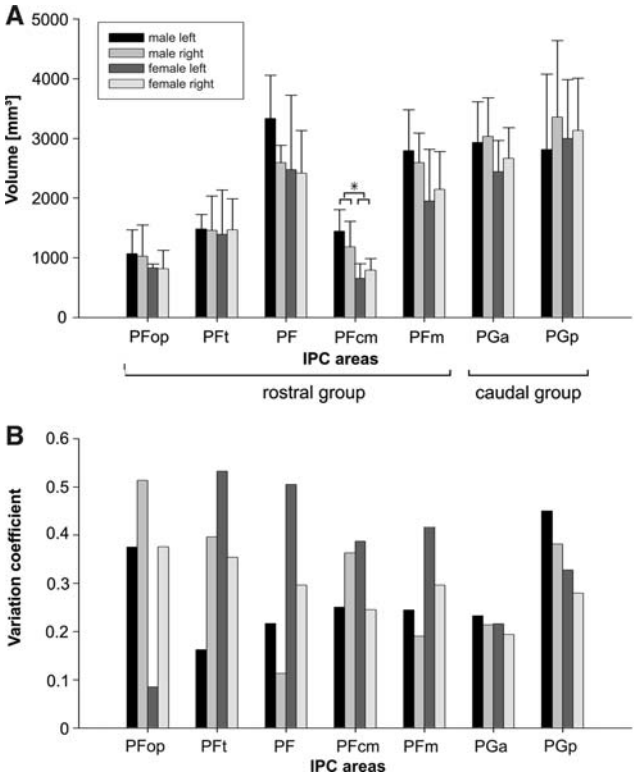

Fig. 7 Vertical bar charts of the volumes (**a**) and variation coefficients (**b**) of the IPC areas. For each IPC area, four bars are plotted: *male left*, *male right*, *female left*, *female right*. Significant gender difference ($P < 0.05$) is marked with an *asterisk*

hIP2 (Choi et al. 2006), two areas of the anterior IPS, shared frequently, but not always a common border with areas PF, PFm, and PGa. The rostral areas PFop, PFt, PF, and PFcm bordered areas OP1–4 of the parietal operculum and the SII cortex (Eickhoff et al. 2006c), but the exact neighbourhood relationships were variable. Area PFop, for example, had common borders with all SII areas, whereas PF only bordered OP1. PFt, on the other hand, was the 'preferred' neighbour of BA2 (Grefkes et al. 2001), connecting the IPL with the somatosensory cortex in the postcentral sulcus.

The Sylvian fissure was a reliable landmark for the ventral extent of the IPL areas. Areas PFop and PFcm were located within the Sylvian fissure; their extent into the dorsal bank of the Sylvian fissure, however, was variable. None of the IPL areas ever reached the insular cortex.

The caudal IPL areas, PGa and PGp, were surrounded by cortex which has not been cytoarchitectonically mapped yet: PGp was found in close proximity to the extrastriate area hOc5 (Malikovic et al. 2007), but another region, yet unmapped, was located between them (Fig. 5). Areas PGa and PGp bordered ventrally uncharted areas at the junction between temporal, parietal and occipital cortex, corresponding to areas 37 and 19 in the map of Brodmann (1909).

The PF and PG areas were mainly located on the supramarginal and the angular gyrus, respectively, but the exact borders between the rostral and caudal part of the IPL could not be identified by pure macroscopical inspection. The border between PFm and PGa were located in some hemispheres within the primary intermediate sulcus (Jenssen sulcus). However, this sulcus was highly variable across the examined brains. The Jenssen sulcus was not present in all examined brains which is in accordance with the literature (Ono et al. 1990); where no Jenssen sulcus was found, the border between rostral and caudal IPL was found either on the free surface of the IPL or in unnamed sulci between supramargnial and angular gyrus (according to Ono et al. 1990). The bipartite parcellation into a rostral area 40 and a caudal area 39, as supposed by Brodmann (1909), was not fully supported by our findings. The differentiation between rostral and caudal IPL was just partially possible by allocating the areas to the supramarginal or angular gyrus. The exact localisation was only possible by microscopical inspection.

Cytoarchitectonical probability maps and variability in stereotaxic space

Intersubject variability in stereotaxic space may be caused by the following factors: the IPL areas belong to association areas for which variability can be assumed to be higher than for primary cortical areas. Fischl et al. (2007) showed that higher order cortical areas exhibited more variability than primary and secondary cortical areas, using the cortical folding pattern as a predictor for the variability of an

Table 5 Gender specific volumetric data of the IPL areas

	Male		Female	
	Left	Right	Left	Right
PFop	1,062 ± 448.5	1,019 ± 589.4	821 ± 83.3	811 ± 344.1
CV	0.42	0.58	0.10	0.42
Ft	1,475 ± 267.2	1,446 ± 626.7	1,385 ± 831.8	1,463 ± 587.7
CV	0.18	0.43	0.60	0.40
PF	3,319 ± 823.4	2,579 ± 331.4	2,464 ± 1404.6	2,407 ± 813.9
CV	0.25	0.13	0.57	0.34
PFm	2,782 ± 772.7	2,582 ± 562.8	1,944 ± 973.9	2,129 ± 708.4
CV	0.28	0.22	0.50	0.33
PFcm	1,436 ± 407.7	1,173 ± 466.3	646 ± 279.4	785 ± 216.6
CV	0.28	0.40	0.43	0.28
PGa	2,910 ± 729.7	3,014 ± 725.1	2,424 ± 592.8	2,646 ± 569.6
CV	0.25	0.24	0.25	0.22
PGp	2,795 ± 1,412.4	3,337 ± 1421.3	2,973 ± 1064.1	3,107 ± 960.5
CV	0.51	0.43	0.36	0.31

Mean volumes (±standard deviations) in mm^3 and variation coefficients (CV) for each IPL area for the group of male and female brains, separately for left and right hemisphere. Individual correction for shrinkage due to histological processing has been performed according to Amunts et al. (2005)

area. The primary cortical areas were best predictable from the corresponding cortical folds and least variable, whereas higher order cortical areas were least predictable and more variable (Fischl et al. 2007).

Another factor influencing intersubject variability is the size of an area. The intersubject variability in the intraparietal areas hIP1 and hIP2 (Choi et al. 2006), for example, was higher than that of area 7A of the superior parietal cortex (Scheperjans et al. 2008). But areas hIP1 and hIP2 were also smaller than area 7A. The same was true for the relatively small area hOc5 (Malikovic et al. 2007) of the extrastriate cortex as compared to V1, the primary visual cortex (Amunts et al. 2000). In addition, the smaller areas (hIP1, hIP2, hOc5) seem to be located in brain regions, where the macroanatomical variability is more pronounced as compared to those regions where some of the larger areas (7A, V1) were found.

Since all IPL areas were higher order cortical areas, the size argument, and not the role in cortical hierarchies seems to be a significant factor, although subtle and yet unknown differences in the hierarchy of the IPL areas, which may interact with the size of the areas cannot be ruled out. The intersubject variability as estimated by the distributions of overlap in the probability maps of the IPL areas mostly resembled those of the somatosensory areas BA 2 (Grefkes et al. 2001) and OP1–OP4 (Eickhoff et al. 2006a) as well as the ventral extrastriate cortex (areas hOc3v, hOc4v; Rottschy et al. 2007). Intersubject variability of IPL areas was higher than that of the allocortical structures amygdala, hippocampus and entorhinal cortex, which showed a high amount of voxels with probabilities of 90 or 100% (Amunts et al. 2005).

Volumetric interhemispheric and gender asymmetries

The volumetric analysis presented in this study was performed on cytoarchitectonically defined areas, delineated in ten human post-mortem brains. The study of Eidelberg and Galaburda (1984) used a comparable cytoarchitectonic approach. The authors identified four different cytoarchitectonic areas on the free surface of the human IPL, which were arranged in a rostro-caudal sequence: PF (∼BA 40), PFG (transition between rostral (BA 40) and caudal (BA 39) IPL, PG (∼BA 39) and OPG (transition to occipital lobe). They analysed the volumes of two of the areas (i.e. the caudal areas PG and OPG) in a sample of eight brains, whereby no significant interhemispheric differences were found. Topographically, these areas approximately match our areas PGa and PGp, which also did not show significant volume differences between left and right hemispheres. Thus, the cytoarchitectonic study of Eidelberg and Galaburda is in accordance with our findings of interhemispheric symmetry of caudal IPL areas in volume. Our study has added findings for the rostral areas, where no interhemispheric differences have been found either. Gender asymmetries have not been analysed in the study of Eidelberg and Galaburda.

To interpret the functional significance of gender differences and interhemispheric asymmetry, imaging studies in healthy volunteers and clinical observations in patients provide further support. We found a significant gender difference for area PFcm, located in the caudal part of the Sylvian fissure which was significantly larger in males than in females. Clinical studies showed that left-hemispheric lesions in this particular region may cause Wernicke's and primary progressive aphasia, as the whole language-system

is mostly left-lateralized (e.g. Amici et al. 2006; Gorno-Tempini et al. 2004; Mesulam 2001; Ojemann 1979). Whereas interhemispheric cytoarchitectonic asymmetries have been found in the anterior language region (Amunts et al. 1999; Galaburda and Geschwind 1980), such differences for the posterior language region including Wernicke's region are sparser (e.g. Witelson and Kigar 1992).

The results of lesion studies concerning gender differences are contradictory: some studies report such differences in the perisylvian region, where men showed more extended lesions in this posterior language area (Lang and Moser 2003). Another study showed that women with primary progressive aphasia were more impaired in speech production than men (Rogalski et al. 2007). A comparable result was found for stroke patients, where women showed aphasic symptoms significantly more frequently than men (Di Carlo et al. 2003). Other studies in aphasics, in contrast, did not find a male or female dominance in this language-related area (e.g. Godefroy et al. 2002; Pedersen et al. 2004). The reported functional gender differences may be correlated with our observed anatomical asymmetry for area PFcm. Further studies, which correlate the anatomical probability maps of the IPL areas with functional imaging data, are needed in order to investigate possible functional correlates concerning these gender differences.

The IPL is involved in different cognitive functions, involving different fronto-parietal and parieto-occipital networks. Some of them show gender and/or hemispheric differences, part of which can be explained by cytoarchitectonic differences (e.g. volume of PFcm). A further approach to investigate interhemispheric cytoarchitectonic differences and their impact on brain function is the application of the cytoarchitectonic stereotaxic maps in functional imaging studies analysing the involvement of IPL areas in different experimental setups, e.g. spatial attention, motor planning and language-related tasks. Further clues may be expected from emerging techniques for analysing anatomical and effective connectivity in the human brain by means of diffusion tensor imaging (DTI) and dynamic causal modelling (DCM), respectively (Friston et al. 2003, Behrens and Johansen-Berg 2005). Considering that function and cytoarchitecture of the parietal cortex cannot be analysed in one and the same human brain, such inter-modal data integration by means of probabilistic atlases represents currently the most straightforward tool for the analysis of the structure–function correspondences in the human brain (Toga et al. 2006). The probability maps of all IPL areas, together with a software tool (Eickhoff et al. 2005) for their integration into the widely used functional image analysis software packages SPM, FSL, and AFNI, are freely available to all researchers at http://www.fz-juelich.de/ime/spm_anatomy_toolbox.

Acknowledgments This work was supported by a grant (to K. Z.) funded by the DFG (grant KFO 112), a Human Brain Project/Neuroinformatics Research grant funded by the National Institute of Biomedical Imaging and Bioengeneering, the National Institute of Neurological Disorders and Stroke, and the National Institute of Mental Health (K. A. and K. Z.), and by a grant (to K. Z.) of the European Commission (Grant QLG3-CT-2002-00746). Further support by the BMBF (BMBF 01GO0104), Brain Imaging Center West (BMBF 01GO0204) is gratefully acknowledged.

References

Abo M, Senoo A, Watanabe S, Miyano S, Doseki K, Sasaki N et al (2004) Language-related brain function during word repetition in post-stroke aphasics. Neuroreport 15(12):1891–1894. doi:10.1097/00001756-200408260-00011

Amici S, Gorno-Tempini ML, Ogar JM, Dronkers NF, Miller BL (2006) An overview on primary progressive aphasia and its variants. Behav Neurol 17(2):77–87

Amunts K, Schleicher A, Bürgel U, Mohlberg H, Uylings HBM, Zilles K (1999) Broca's region revisited: cytoarchitecture and intersubject variability. J Comp Neurol 412:319–341. doi:10.1002/(SICI)1096-9861(19990920)412:2<319::AID-CNE10>3.0.CO;2-7

Amunts K, Malikovic A, Mohlberg H, Schormann T, Zilles K (2000) Brodmann's areas 17 and 18 brought into stereotaxic space—where and how variable? Neuroimage 11:66–84. doi:10.1006/nimg.1999.0516

Amunts K, Kedo O, Kindler M, Pieperhoff P, Mohlberg H, Shah NJ et al (2005) Cytoarchitectonic mapping of the human amygdala, hippocampal region and the entorhinal cortex: intersubject variability and probability maps. Anat Embryol (Berl) 210:343–352. doi:10.1007/s00429-005-0025-5

Amunts K, Armstrong E, Malikovic A, Hömke L, Mohlberg H, Schleicher A et al (2007a) Gender-specific left-right asymmetries in human visual cortex. J Neurosci 27(6):1356–1364. doi:10.1523/JNEUROSCI.4753-06.2007

Amunts K, Schleicher A, Zilles K (2007b) Cytoarchitecture of the cerebral cortex—more than localization. Neuroimage 37(4):1061–1065. doi:10.1016/j.neuroimage.2007.02.037

Astafiev SV, Shulman GL, Stanley CM, Snyder AZ, Van Essen DC, Corbetta M (2003) Functional organization of human intraparietal and frontal cortex for attending, looking and pointing. J Neurosci 23(11):4689–4699

Batsch EG (1956) Die myeloarchitektonische Untergliederung des Isocortex parietalis beim Menschen. J Hirnforsch 2:225–258

Behrens TE, Johansen-Berg H (2005) Relating connectional architecture to grey matter function using diffusion imaging. Philos Trans R Soc Lond B Biol Sci 360:903–911. doi:10.1098/rstb.2005.1640

Bell EC, Wilson MC, Wilman AH, Dave S, Silverstone PH (2006) Males and females differ in brain activation during cognitive tasks. Neuroimage 30(2):529–538. doi:10.1016/j.neuroimage.2005.09.049

Blank SC, Scott SK, Murphy K, Warburton E, Wise RJ (2002) Speech production: Wernicke, Broca and beyond. Brain 125:1829–1838. doi:10.1093/brain/awf191

Boghi A, Rasetti R, Avidano F, Manzone C, Orsi L, D'Agata F et al (2006) The effect of gender on planning: an fMRI study using the Tower of London task. Neuroimage 33(3):999–1010. doi:10.1016/j.neuroimage.2006.07.022

Brodmann K (1909) Vergleichende Lokalisationslehre der Großhirnrinde. Barth, Leipzig

Caspers S, Geyer S, Schleicher A, Mohlberg H, Amunts K, Zilles K (2006) The human inferior parietal lobule: cytoarchitectonic parcellation and interindividual variability. Neuroimage 33(2): 430–448. doi:10.1016/j.neuroimage.2006.06.054

Choi HJ, Zilles K, Mohlberg H, Schleicher A, Fink GR, Armstrong E et al (2006) Cytoarchitectonic identification and probabilistic mapping of two distinct areas within the anterior ventral bank of the human intraparietal sulcus. J Comp Neurol 495(1):53–69. doi:10.1002/cne.20849

Chung SC, Sohn JH, Lee B, Tack GR, Yi JH, You JH et al (2007) A comparison of the mean signal change method and the voxel count method to evaluate the sensitivity of individual variability in visuospatial performance. Neurosci Lett 418(2):138–142. doi: 10.1016/j.neulet.2007.03.014

Collins DL, Neelin P, Peters TM, Evans AC (1994) Automatic 3D intersubject registration of MR volumetric data in standardized Talairach space. J Comput Assist Tomogr 18:192–205. doi: 10.1097/00004728-199403000-00005

Corbetta M, Shulman GL (2002) Control of goal-directed and stimulus-driven attention in the brain. Nat Neurosci Rev 3:201–215. doi:10.1038/nrn755

Di Carlo A, Lamassa M, Baldereschi M, Pracucci G, Basile AM, Wolfe CD, et al., European BIOMED Study of Stroke Care Group (2003) Sex differences in the clinical presentation, resource use, and 3-month outcome of acute stroke in Europe: data from a multicenter multinational hospital-based registry. Stroke 34(5): 1114–1119. doi:10.1161/01.STR.0000068410.07397.D7

Eickhoff S, Stephan KE, Mohlberg H, Grefkes C, Fink GR, Amunts K et al (2005) A new SPM toolbox for combining probabilistic cytoarchitectonic maps and functional imaging data. Neuroimage 25:1325–1335. doi:10.1016/j.neuroimage.2004.12.034

Eickhoff S, Amunts K, Mohlberg H, Zilles K (2006a) The human parietal operculum. II. Stereotaxic maps and correlation with functional imaging results. Cereb Cortex 16:268–279. doi: 10.1093/cercor/bhi106

Eickhoff SB, Heim S, Zilles K, Amunts K (2006b) Testing anatomically specified hypotheses in functional imaging using cytoarchitectonic maps. Neuroimage 32:570–582. doi:10.1016/j.neuroimage.2006.04.204

Eickhoff S, Schleicher A, Zilles K, Amunts K (2006c) The human parietal operculum. I. Cytoarchitectonic mapping of subdivisions. Cereb Cortex 16:254–267. doi:10.1093/cercor/bhi105

Eidelberg D, Galaburda AM (1984) Inferior parietal lobule—divergent architectonic asymmetries in the human brain. Arch Neurol 41(8):843–852

Evans AC, Marrett S, Neelin P, Collins L, Worsley K, Dai W et al (1992) Anatomical mapping of functional activation in stereotaxic coordinate space. Neuroimage 1:43–53

Fink GR, Heide W (2004) Spatial neglect. Nervenarzt 75(4):389–408. doi:10.1007/s00115-004-1698-3

Fischl B, Rajendran N, Busa E, Augustinack J, Hinds O, Yeo BT et al. (2007) Cortical folding patterns and predicting cytoarchitecture. Cereb Cortex (in press). doi:10.1093/cercor/bhm225

Friston KJ, Harrison L, Penny W (2003) Dynamic causal modelling. Neuroimage 19(4):1273–1304. doi:10.1016/S1053-8119(03)00202-7

Galaburda AM, Geschwind N (1980) The human language areas and cerebral asymmetries. Rev Med Suisse Romande 100(2):119–128

Gerhardt E (1940) Die Cytoarchitektonik des Isocortex parietalis beim Menschen. J Psychol Neurol 49:367–419

Geyer S (2004) The microstructural border between the motor and the cognitive domain in the human cerebral cortex. Advances in anatomy embryology and cell biology, vol 174. Springer, Berlin

Geyer S, Ledberg A, Schleicher A, Kinomura S, Schormann T, Bürgel U et al (1996) Two different areas within the primary motor cortex of man. Nature 382:805–807. doi:10.1038/382805a0

Geyer S, Schormann T, Mohlberg H, Zilles K (2000) Areas 3a, 3b, and 1 of human primary somatosensory cortex. Part 2: spatial normalization to standard anatomical space. Neuroimage 11:684–696. doi:10.1006/nimg.2000.0548

Godefroy O, Dubois C, Debachy B, Leclerc M, Kreisler A, Lille Stroke Program (2002) Vascular aphasias: main characteristics of patients hospitalized in acute stroke units. Stroke 33(3):702–705. doi:10.1161/hs0302.103653

Gorno-Tempini ML, Dronkers NF, Rankin KP, Ogar JM, Phengrasamy L, Rosen HJ et al (2004) Cognition and anatomy in three variants of primary progressive aphasia. Ann Neurol 55(3):335–346. doi:10.1002/ana.10825

Grefkes C, Geyer S, Schormann T, Roland P, Zilles K (2001) Human somatosensory area 2: oberserver-independent cytoarchitectonic mapping, interindividual variability, and population map. Neuroimage 14:617–631. doi:10.1006/nimg.2001.0858

Halligan PW, Fink GR, Marshall JC, Vallar G (2003) Spatial cognition: evidence from visual neglect. Trends Cogn Sci 7(3):125–133. doi:10.1016/S1364-6613(03)00032-9

Hesse MD, Thiel CM, Stephan KE, Fink GR (2006) The left parietal cortex and motor intention: an event-related functional magnetic resonance imaging study. Neurosci 140:1209–1221. doi:10.1016/j.neuroscience.2006.03.030

Hömke L (2006) A multirigid method for anisotropic PDE's in elastic image registration. Numer Linear Algebra Appl 13(2–3):215–229. doi:10.1002/nla.477

Holmes CJ, Hoge R, Collins L, Woods R, Toga AW, Evans AC (1998) Enhancement of MR images using registration for signal averaging. J Comput Assist Tomogr 22:324–333. doi:10.1097/00004728-199803000-00032

Jodzio K, Gasecki D, Drumm DA, Lass P, Nyka W (2003) Neuroanatomical correlates of the post-stroke aphasias studied with cerebral blood flow SPECT scanning. Med Sci Monit 9(3):32–41

Kerkhoff G (2001) Spatial hemineglect in humans. Prog Neurobiol 63(1):1–27. doi:10.1016/S0301-0082(00)00028-9

Kertesz A, Benke T (1989) Sex equality in intrahemispheric language organization. Brain Lang 37(3):401–408. doi:10.1016/0093-934X(89)90027-8

Kimura D (1983) Sex differences in cerebral organization for speech and praxic function. Can J Psychol 37(1):19–35. doi:10.1037/h0080696

Lang CJ, Moser F (2003) Localization of cerebral lesions in aphasia—a computer aided comparison between men and women. Arch Women Ment Health 6(2):139–145. doi:10.1007/s00737-003-0166-6

Lendrem W, Lincoln NB (1985) Spontaneous recovery of language in patients with aphasia between 4 and 34 weeks after stroke. J Neurol Neurosurg Psychiatry 48(8):743–748

Malikovic A, Amunts K, Schleicher A, Mohlberg H, Eickhoff SB, Wilms M et al (2007) Cytoarchitectonic analysis of the human extrastriate cortex in the region V5/MT+: a probabilistic, stereotaxic map of area hOc5. Cereb Cortex 17(3):562–574. doi: 10.1093/cercor/bhj181

Marshall JC, Fink GR (2001) Spatial cognition: where we were and where we are. Neuroimage 14:2–7. doi:10.1006/nimg.2001.0834

Mesulam MM (2001) Primary progressive aphasia. Ann Neurol 49(4):425–432. doi:10.1002/ana.91

Miceli G, Caltagirone C, Gainotti G, Masullo C, Silveri MC, Villa G (1981) Influence of age, sex, literacy and pathologic lesion on incidence, severity and type of aphasia. Acta Neurol Scand 64(5):370–382

Morosan P, Rademacher J, Schleicher A, Amunts K, Schormann T, Zilles K (2001) Human primary auditory cortex: cytoarchitectonic

subdivisions and mapping into a spatial reference system. Neuroimage 13:684–701. doi:10.1006/nimg.2000.0715
Ojemann GA (1979) Individual variability in cortical localization of language. J Neurosurg 50(2):164–169
Ono M, Kubik S, Abernathey CD (1990) Atlas of the cerebral sulci. Thieme, Stuttgart
Pedersen PM, Vinter K, Olsen TS (2004) Aphasia after stroke: type, severity and prognosis. The Copenhagen aphasia study. Cerebrovasc Dis 17(1):35–43. doi:10.1159/000073896
Rogalski E, Rademacher A, Weintraub S (2007) Primary progressive aphasia: relationship between gender and severity of language impairment. Cogn Behav Neurol 20(1):38–43. doi:10.1097/WNN.0b013e31802e3bae
Rottschy C, Eickhoff SB, Schleicher A, Mohlberg H, Kújovic M, Zilles K et al (2007) The ventral visual cortex in humans: cytoarchitectonic mapping of two extrastriate areas. Hum Brain Mapp 28(10):1045–1059. doi:10.1002/hbm.20348
Rushworth M, Ellison A, Walsh V (2001a) Complementary localization and lateralization of orienting and motor attention. Nat Neurosci 4(6):656–661. doi:10.1038/88492
Rushworth M, Krams M, Passingham RE (2001b) The attentional role of the left parietal cortex: the distinct lateralization and localization of motor attention in the human brain. J Cogn Neurosci 13(5):698–710. doi:10.1162/089892901750363244
Sarkissov SA, Filimonoff IN, Kononowa EP, Preobraschenskaja IS, Kukuew LA (1955) Atlas of the cytoarchitectonics of the human cerebral cortex (Russian). Medgiz, Moscow
Scheperjans F, Eickhoff SB, Hömke L, Mohlberg H, Hermann K, Amunts K, et al. (2008) Probabilistic maps, morphometry, and variability of cytoarchitectonic areas in the human superior parietal cortex. Cereb Cortex (in press). doi:10.1093/cercor/bhm241
Schleicher A, Palomero-Gallagher N, Morosan P, Eickhoff SB, Kowalski T, de Vos K et al (2005) Quantitative architectural analysis: a new approach to cortical mapping. Anat Embryol (Berl) 210(5):373–386. doi:10.1007/s00429-005-0028-2
Smith BD, Meyers M, Kline R, Bozman A (1987) Hemispheric asymmetry and emotion: lateralized parietal processing of affect and cognition. Biol Psychol 25(3):247–260. doi:10.1016/0301-0511(87)90050-0
Sugiura M, Friston KJ, Wilmes K, Shah NJ, Zilles K, Fink GR (2007) Analysis of intersubject variability in activation: an application to the incidental episodic retrieval during recognition test. Hum Brain Mapp 28(1):49–58. doi:10.1002/hbm.20256
Talairach J, Tournoux P (1988) Co-planar stereotaxic atlas of the human brain. Thieme, Stuttgart
Toga AW, Thompson PM, Mori S, Amunts K, Zilles K (2006) Towards multimodal atlases of the human brain. Nat Rev Neurosci 7:952–966. doi:10.1038/nrn2012
Tzourio-Mazoyer N, Josse G, Crivello F, Mazoyer B (2004) Interindividual variability in the hemispheric organization for speech. Neuroimage 21(1):422–435. doi:10.1016/j.neuroimage.2003.08.032
Vallar G (2001) Extrapersonal visual unilateral spatial neglect and its neuroanatomy. Neuroimage 14:52–58. doi:10.1006/nimg.2001.0822
Vesia M, Monteon JA, Sergio LE, Crawford JD (2004) Hemispheric asymmetry in memory-guided pointing during single-pulse transcranial magnetic stimulation of human parietal cortex. J Neurophysiol 96(6):3016–3027. doi:10.1152/jn.00411.2006
Vogt C, Vogt O (1919) Allgemeinere Ergebnisse unserer Hirnforschung. J Psychol Neurol 25:279–461
von Economo K, Koskinas G (1925) Die Cytoarchitektonik der Hirnrinde des erwachsenen Menschen. Springer, Wien
Witelson SF, Kigar DL (1992) Sylvian fissure morphology and asymmetry in men and women: bilateral differences in relation to handedness in men. J Comp Neurol 323(3):326–340. doi:10.1002/cne.903230303
Zilles K, Armstrong E, Schleicher A, Kretschmann HJ (1988) The human pattern of gyrification in the cerebral cortex. Anat Embryol (Berl) 179(2):173–179. doi:10.1007/BF00304699
Zilles K, Schleicher A, Palomero-Gallagher N, Amunts K (2002) Quantitative analysis of cyto- and receptorarchitecture of the human brain. In: Toga AW, Mazziotta JC (eds) Brain mapping: the methods, 2nd edn. Academic Press, New York, pp 573–602